Artifact Detection of Wrist Photoplethysmograph Signals

Kaat Vandecasteele[1,2], Jesús Lázaro[1,2], Evy Cleeren[3], Kasper Claes[4], Wim Van Paesschen[3], Sabine Van Huffel[1,2] and Borbála Hunyadi[1,2]

[1]*KU Leuven, Department of Electrical Engineering (ESAT), STADIUS Center for Dynamical Systems, Signal Processing and Data Analytics, Leuven, Belgium*

[2]*imec, Leuven, Belgium*

[3]*KU Leuven, University Hospital, Department of Neurosciences, Leuven, Belgium*

[4]*UCB, Brussels, Belgium*

Keywords: Artifact Detection, Photoplethysmography, Wrist, Feature Selection.

Abstract: There is a growing interest in monitoring of vital signs through wearable devices, such as heart rate (HR). A comfortable and non-invasive technique to measure the HR is pulse photoplethysmography (PPG) with the use of a smartwatch. This watch records also triaxial accelerometry (ACM). However, it is well known that motion and noise artifacts (MNA) are present. A MNA detection method, which classifies into a clean or MNA segment, is trained and tested on a dataset of 17 patients, each with a recording duration of 24 hours. PPG- and ACM-derived features are extracted and classified with a LS-SVM classifier. A sensitivity and specificity of respectively 85.50 % and 92.36 % are obtained. For this dataset, the ACM features do not improve the performance, suggesting that ACM recording could be avoided from the point of view for detecting MNA in PPG signals during daily life.

1 INTRODUCTION

There is a growing interest in wearable and continuous monitoring of vital signs, such as heart rate (HR). A comfortable and non-invasive technique to measure the HR is pulse photoplethysmography (PPG). PPG makes use of reflected or transmitted light through the skin to measure a pulsatile physiological waveform caused by changes in the blood volume due to a heart beat. Common PPG recording locations include fingers, ears, toes, forehead or wrist (Allen, 2007). The wrist is a possible recording location. An advantage is that the PPG sensor can be embedded in a watch. However, it is well known that motion and noise artifacts (MNA) can distort the signal (Petterson et al., 2007). Those MNA are caused by 1) the movement of venous blood as well as other non-pulsatile components 2) variations in the optical coupling between the sensor and the skin (Barker and Shah, 1997; Tobin et al., 2002). The MNA can be particularly challenging when computing derived features from the PPG waveform such as HR. Various design approaches to reduce MNA have been proposed (Li and Warren, 2012). With these improvements, MNA are stil present. Therefore, algorithm-based MNA reduction methods were proposed (Torres et al., 2016; Lai and Kim, 2015; Fukushima et al., 2012; Pan et al., 2016; Torres et al., 2016; Yousefi et al., 2012; Ram et al., 2012; Lee et al., 2010; Temko, 2017; Torres et al., 2016; Kim and Yoo, 2006). These MNA reduction algorithms operate also on clean parts of the signal, which is unnecessary computation and can cause distortion of the signal. Therefore an algorithm which can distinguish clean parts from MNA is desired. MNA detection algorithms are designed with the use of waveform morphologies (Sukor et al., 2011; Li et al., 2012; Li et al., 2008; Fischer et al., 2017) or filtered output (Nakajima et al., 1996; Karlen et al., 2012). Statistical measures, such as skewness, kurtosis, shannon entropy and Renyi's entropy have been shown useful for automatic detection of MNA (Selvaraj et al., 2011; Krishnan et al., 2008). Another approach, using Hjorth parameters was proposed (Gil et al., 2008). Other methods were published, which perform classification with a support vector machine (SVM) with time-domain features (Chong et al., 2014) or time-frequency spectrum analysis (Dao et al., 2016) .

To the best of our knowledge, all these methods are tested and validated for PPG recorded on the ears,

Vandecasteele, K., Lázaro, J., Cleeren, E., Claes, K., Paesschen, W., Huffel, S. and Hunyadi, B.
Artifact Detection of Wrist Photoplethysmograph Signals.
DOI: 10.5220/0006594301820189
In *Proceedings of the 11th International Joint Conference on Biomedical Engineering Systems and Technologies (BIOSTEC 2018) - Volume 4: BIOSIGNALS*, pages 182-189
ISBN: 978-989-758-279-0

fingers or forehead, but none have been validated on the wrist. Moreover, these methods are never tested on 24 hour recordings. In our paper, we propose an automated computer-based method for the detection of MNA in PPG signals, recorded with a wrist watch. The method is validated on 24-hour data recordings. The classification is performed with a LS-SVM model using previously published features (Selvaraj et al., 2011; Gil et al., 2008; Chong et al., 2014), together with new features. Additional to the PPG signals, most smart watches also record the accelerometry (ACM). Therefore, it is investigated if the ACM improves the MNA detection method. A backwards wrapper feature selection is implemented to determine which features are the most discriminative ones. The goal of the paper is to provide a reliable MNA detection method, validated for wrist PPG signals, and additionally to evaluate whether the ACM improves the detection performance.

2 METHODOLOGY

The methodology consists of five parts. Firstly, the data collection is described. Secondly, the extracted features from the PPG signal, are summarized. Thirdly, a LS-SVM-based classifier is discussed. Fourthly, a feature selection method is explained, which selects the most discriminative features. Lastly, the labelling process is explained. With the use of a reference signal, a label (Clean or MNA) is given to each PPG segment.

2.1 Data Acquisition

The dataset, used in this experiment, contains recordings of 17 epilepsy patients, each with a duration around 24 hours. The epilepsy patients were recorded with a wired conventional multi-channel scalp EEG. Additionally to the standard clinical equipment, recordings were made with a wearable ECG device: the 180^o eMotion Faros (Bittium Biosignals Ltd, 2017), and a wrist-worn PPG device: the E4 Empatica wristband (Empatica Inc, 2017). The Faros ECG was used in a single-channel configuration. The Empatica E4 measures reflective PPG using a green and a red LED on the wrist. The device returns a single channel which is obtained by combining the green and the red channels using Empatica's proprietary algorithm. Additional to the 1-channel PPG, the triaxial ACM is recorded. Considering that the intravenous insertion, used to administer medication in clinical practice, is routinely placed at the non-dominant wrist, the patients wore the Empatica watch on the dominant hand. The sampling rate of the Faros and Empatica (PPG/ACM) device are respectively 500Hz and 64Hz (PPG)/32 Hz (ACM).

2.2 Feature Extraction

Features are extracted from both the PPG signal and ACM signal. Features from literature, which are previously shown to be useful, are combined with our own features. First, the PPG signal was preprocessed by a 5th order bandpass butterworth filter [0.5 - 12 Hz]. The ACM was preprocessed by a 3th order butterworth filter [0.2 - 10Hz]. The PPG signal and corresponding ACM data are segmented in 7 seconds, because it was reported to be the optimal segment length for MNA detection (Chong et al., 2014).

2.2.1 PPG

The following features were extracted from the PPG segments:

- Standard Deviation of Pulse-to-Pulse Interval (STD_{HR}), Standard Deviation of Pulse-to-Pulse Amplitude (STD_{amp}), Standard Deviation of Systolic and Diastolic Ratio (STD_{SD}) and Mean-Standard Deviation of Pulse Shape (STD_{WAV}), which are described in (Chong et al., 2014)
- Kurtosis (K) and Shannon Entropy (SE), which are described in (Selvaraj et al., 2011)
- Variance (Var) of the signal segment
- The frequency of the first/second/third-largest peak in the power spectrum (FLP/SLP/TLP), which are expected to be around 1Hz (the HR frequency)/ 2Hz (the first harmonic)/ 3Hz (the second harmonic) for a clean segment
- Spectral Shannon entropy (SSE), which is the shannon entropy of the power spectrum
- Hjorth parameters: H1 and H2, which represents respectively the central frequency and half of the bandwidth (Gil et al., 2008)

In order to calculate the features STD_{HR} and STD_{amp}, the location and amplitude of the pulse peaks are needed. The feature STD_{SD} requires the systolic and diastolic time, which are respectively the rising time from valley to peak and the falling time from peak to the next valley. The feature STD_{WAV} require the alignment of the pulses in a segment, which is done with the peak location. To calculate the location and amplitude of the pulse peaks and pulse valleys, an algorithm developed in (Lázaro et al., 2014) is used. This algorithm consists of two phases: a linear filtering transformation and an adaptive thresholding

operation. The filtering step consists of a linear-phase FIR low-pass-differentiator filter, which is used to accentuate the abrupt upslopes of the PPG pulses. The abrupt upslopes correspond to peaks in the filtered signal, which are detected by an adaptive thresholding operation. Once the peaks in the filtered signal are found, the maximum and minimum point in the original PPG signal are found.

2.2.2 ACM

The following features were extracted from each direction and Euclidean norm of the ACM segments:

1. The maximal value of the rectified segment (max_x,max_y,max_z and max_{norm})
2. The 90th percentile of the rectified segment (90_x,90_y,90_z and 90_{norm})
3. The Variance of the segment (Var_x,Var_y,Var_z and Var_{norm})
4. The mean absolute deviation of the segment (MAD_x,MAD_y,MAD_z and MAD_{norm})
5. The norm of the segment ($Norm_x$,$Norm_y$,$Norm_z$ and $Norm_{norm}$)

2.3 LS-SVM based Classification of MNA

The classification is done with a LS-SVM (Least Squares Support Vector Machines) classifier (De Brabanter et al., 2003) using a linear kernel. The classifier is trained and tested within a leave-one-patient-out cross-validation (LOPO-CV) approach. In this way, no data of the patient itself is used for the training. To evaluate the classifier, the sensitivity (proportion of MNA segments that are correctly classified), the specificity (the proportion of clean segments that are correctly classified) and the accuracy are calculated. The classifier is tested with only PPG features, only ACC features and all the features together.

2.4 Feature Selection

In order to investigate which features are discriminative for clean and MNA PPG segments, a backwards wrapper feature selection method is implemented. In Figure 1 a flow diagram of the method is shown. At the start, the total feature set is used to train and test the classifier within a LOPO-CV approach. As evaluation criteria, the F1-score is calculated, which is the harmonic mean of the sensitivity and the specificity. In a next step, new feature sets are created by leaving out each feature one time. So, if there are N features, N new feature sets are created. Again the classifier is trained and tested with these new feature sets within a LOPO-CV approach and the F1-scores are calculated. Next, the maximal F1-score, corresponding to the best new feature set, is compared with the original F1-score. If this F1-score is higher or equal, this feature doesn't improve the classification problem and is removed. Whole the procedure is calculated again by starting with the new feature set, corresponding to the highest F1-score. With every iteration only 1 feature can be removed. The method will stop when all the new F1-scores are lower.

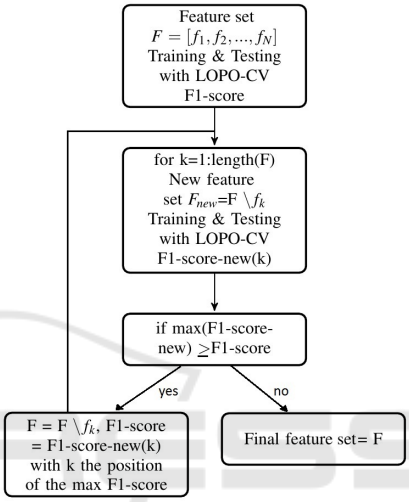

Figure 1: Flowchart: Backwards wrapper feature selection.

The feature selection procedure was performed on the PPG features, ACM features and all the features together.

2.5 Reference Signal: ECG

In order to train and test a classifier, labels for each segment are needed. A visual reference is avoided because it's very subjective, i.e. different visual inspectors annotate the segments differently. Furthermore, it would be very time consuming to annotate a whole dataset of 408 hours (17*24 hours). Instead, we performed an automatic labelling procedure based on the reference electrocardiography (ECG) signal, similarly as in (Chong et al., 2014). The heart rate variability (HRV) is calculated, by finding the location of the R-peaks (Varon et al., 2015). For each PPG segment and corresponding ECG segment, the mean RR-interval (RR_{ECG}) and mean PP-interval (PP_{PPG}) and standard deviation of the RR- and PP-interval (STD_{ECG} and STD_{PPG}) are calculated. A segment is classified as MNA, if $|RR_{ECG} - PP_{PPG}| > 150ms$ or $|STD_{ECG} - STD_{PPG}| > 100ms$. These thresholds are set empirically based on a subset of the data.

3 RESULTS AND DISCUSSION

3.1 Feature Selection

In table 1, 2 and 3 the selected features are shown in bold, starting from respectively the PPG, ACM and all the features. From the newly proposed PPG features, 3 features are retained by the feature selection: the variance, the frequency of the second and third largest peak in the power spectrum. These 3 features do have an added value for the MNA detection algorithm. The feature selection process with the ACM features shows that all features which make use of the y-direction are left out. The y-direction is the direction along the lower arm, from wrist towards the elbow, as shown in Fig. 2. The accelerometry in this direction doesn't have an added value for the algorithm for this dataset.

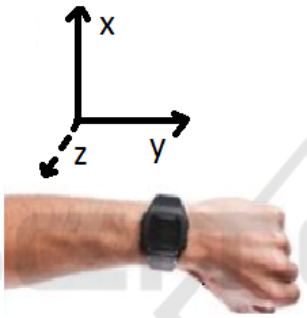

Figure 2: ACM axis.

It might be that motion in the y-direction, which is along the direction of the lower arm, causes less MNA than the other directions. Another reason can be that this direction is less present during daily motion compared to the other directions. The feature selection process with all the features shows that 4 from the 13 PPG-derived and 10 from the 20 ACM-derived features are removed. It seems that the ACM-features have an added value, but this added value is only minor. With all the resulting features, a F1-score of 0.8841 is obtained. If 1 of those PPG-derived features is removed, a F1-score between 0.8474 and 0.8836 is obtained. If one of the ACM-derived features is removed, a F1-score between 0.8831 and 0.8841 is obtained. So leaving out a ACM-feature would only decrease the F1-score slightly.

3.2 Classification Performance

In Figure 3 the sensitivities (Sens), specificities (Spec) and accuracies (Acc) are plotted for all the patients. The sensitivity (specificity) is the proportion of MNA (clean) segments that are correctly classified.

Table 1: Feature selection PPG.

STD_{HR}, **STD_{amp}**, **STD_{SD}** and **STD_{WAV}**
K and SE
Var
FLP, **SLP** and **TLP**
SSE
H1 and H2

Table 2: Feature selection ACC.

max_x, max_y, max_z and **max_{norm}**
90_x, 90_y, **90_z** and **90_{norm}**
Var_x, Var_y, **Var_z** and **Var_{norm}**
MAD_x, MAD_y, **MAD_z** and **MAD_{norm}**
$Norm_x$, $Norm_y$, $Norm_z$ and **$Norm_{norm}$**

Table 3: Feature selection ALL.

STD_{HR}, **STD_{amp}**, **STD_{SD}** and **STD_{WAV}**
K and SE
Var
FLP, **SLP** and **TLP**
SSE
H1 and H2
max_x, max_y, max_z and **max_{norm}**
90_x, **90_y**, **90_z** and **90_{norm}**
Var_x, Var_y, Var_z and Var_{norm}
MAD_x, MAD_y, **MAD_z** and **MAD_{norm}**
$Norm_x$, $Norm_y$, **$Norm_z$** and **$Norm_{norm}$**

The accuracy is the proportion of segments that are correctly classified. In Table 4 the average values $\pm$ standard deviations are shown.

The performance with PPG features is similar as the performance with all features. Adding the ACM features to the classification does not increase the performance. The reason is that the PPG signal has already enough information on itself. The MNA segments show large differences with clean segments, which is illustrated in Figure 4.

By using only the ACM features, a low sensitivity is obtained. This is due to the fact that not all kind of MNA are caused by wrist motion. For example subtle finger motion, which is shown in Figure 5, or bad positioning of the sensor cause MNA, but there is no corresponding ACM activation.

In table 5 previous experiments and results from literature are summarized. In all the studies reflective PPG with infrared light is recorded. The dataset and sensor type are different for each study, which makes it difficult to compare quantitatively the results.

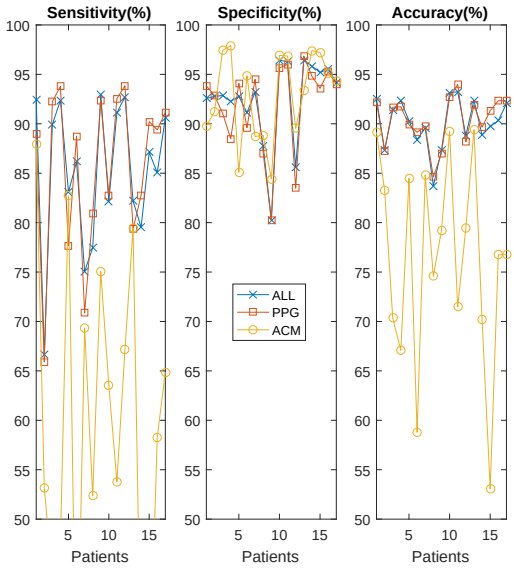

Figure 3: Classification performance.

Table 4: Classification performance.

	PPG	ACM	ALL
Sens (%)	85.50 ± 8	58.04 ± 18	85.50 ± 7
Spec (%)	91.84 ± 5	93.01 ± 4	92.36 ± 4
Acc (%)	90.33 ± 2	76.23 ± 11	90.23 ± 3

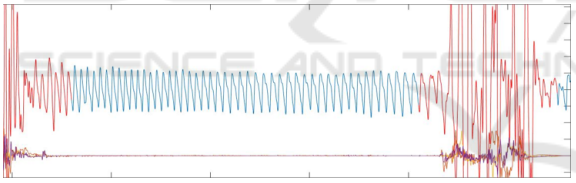

Figure 4: Example: Clean (blue) and MNA (red) PPG segments with 3 axis ACM.

3.3 Overall Data Quality

In total 44.26% ± 16.20% of the data is labeled as MNA based on the reference signal, 43.38% ± 15.62% of the data is detected as MNA by the algorithm. This means that close to half of the measured data are contaminated with MNA, so that the heart rate variability cannot be reliably estimated by the algorithm (Lázaro et al., 2014) from the recorded signals. Note that our dataset was acquired from patients in a hospital environment. The patients are continuously monitored with wired EEG, which limit their mobility. Outside the hospital these percentages are probably even higher.

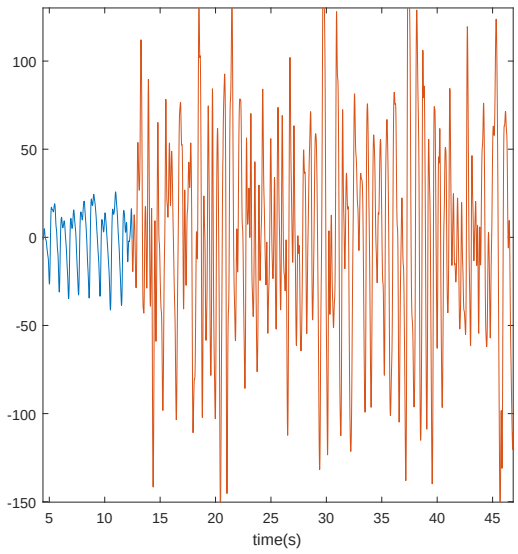

Figure 5: Example: Clean (blue) and MNA, caused by finger motion, (red) PPG.

3.4 Limitations and Further Work

The algorithm is tested on a data set, recorded in the hospital. The algorithm should also be tested on daily life data, recorded outside the hospital.

Only one type of sensor is tested (wrist reflective PPG). It should be extended to other sensors. In order to compare the different studies, the MNA detection algorithms should be tested on the same data sets.

The MNA detection method, explained in this paper, makes use of a fixed window length of 7s. A method should be investigated to automatically determine the length of the MNA.

Other models should be tested for this classification problem, for example deep neural networks.

Extracting HR and HRV is more challenging during these artifactual segments and further signal processing techniques are needed. Further studies must be elaborated to assess how these MNA affect to the different HRV indices.

4 CONCLUSIONS

The goal of the paper is to provide a reliable motion and noise artifact (MNA) detection method for PPG signals, recorded with a wrist watch. PPG- and ACM-derived features are extracted and classified with a LS-SVM classifier. For this dataset, the ACM features do not improve the performance, suggesting that ACM recording could be avoided from the point of view for detecting MNAs in PPG signals.

Table 5: Comparison with literature [Rec.=Recording, Acc=Accuracy, Se=Sensitivity, Sp=Specificity, Results are in %].

No. subjects (Rec. duration)	Sensor type	Type of movement	Results
Sukor et al., 2011			
13 (8 min)	Finger	Hand movements	Acc: 83 ± 11 Se: 89 ± 10 Sp: 77 ± 19
Selvaraj et al., 2011			
10 (5 - 20 min)	Ear/ Finger/ Forehead	Involuntary movements	Acc: 99.0/94.8/93.3 Se: 100/99.3/96.3 Sp: 98.9/93.8/91.9
14 (10 min)	Finger	Voluntary movements	Acc: 88.8 Se: 86.9 Sp: 98.3
Chong et al., 2014			
11 (10 min)	Forehead	Head movement	Acc: 94.4 ± 3.3 Se: 94.7 ± 3.4 Sp: 94.7 ± 4.5
9 (10 min)	Finger	Finger movement	Acc: 93.4 ± 3.5 Se: 88.8 ± 7.9 Sp: 96.7 ± 3.0
9 (45 min)	Finger/Forehead	Stair-climbing	Acc: 93.7 ± 2.7 Se: 93.9 ± 5.0 Sp: 91.4 ± 2.0
Dao et al., 2016			
11 (10 min)	Forehead	Head movement	Acc: 95.7 ± 0.82 Se: 93.0 ± 5.75 Sp: 96.6 ± 1.48
11 (10 min)	Finger	Finger movement	Acc: 97.5 ± 1.50 Se: 96.4 ± 2.34 Sp: 98.1 ± 1.43
10	Forehead	UMMC hospital	Acc: 95.3 ± 1.34 Se: 90.8 ± 2.83 Sp: 98.7 ± 1.07
10	Finger	UMMC hospital	Acc: 94.3 ± 1.64 Se: 88.5 ± 2.23 Sp: 96.9 ± 1.86

ACKNOWLEDGEMENTS

SeizeIT is a project realized in collaboration with imec. Project partners are KU Leuven, UCB Pharma, Byteflies and Pilipili, with project support from VLAIO (Flanders Innovation and Entrepreneurship) and Innoviris.

Bijzonder Onderzoeksfonds KU Leuven (BOF): SPARKLE Sensor-based Platform for the Accurate and Remote monitoring of Kinematics Linked to E-health #: IDO-13-0358; The effect of perinatal stress on the later outcome in preterm babies #: C24/15/036; TARGID - Development of a novel diagnostic medical device to assess gastric motility #: C32-16-00364. Agentschap Innoveren & Ondernemen (VLAIO): Project #: STW 150466 OSA +, O&O HBC 2016 0184 eWatch. iMinds Medical Information Technologies: Dotatie-Strategisch basis onderzoek (SBO- 2016); ICON: HBC.2016.0167 SeizeIT. European Research Council: The research leading to these results has received funding from the European Research Council under the European Union's Seventh Framework Programme (FP7/2007-2013) / ERC Advanced Grant: BIOTENSORS (n^o 339804). This paper reflects only the authors' views and the Union is not liable for any use that may be made of the contained information.

REFERENCES

Allen, J. (2007). Photoplethysmography and its application in clinical physiological measurement. *Physiol. Meas.*, 28(3):R1–R39.

Barker, S. and Shah, N. (1997). The effects of motion on the performance of pulse oximeters in volunteers (revised publication). *Anesthesiology*, (86):101–108.

Bittium Biosignals Ltd (2017). eMotion Faros 180. http://www.megaemg.com/products/faros/. [Online; accessed 22-August-2017].

Chong, J. W., Dao, D. K., Salehizadeh, S. M., McManus, D. D., Darling, C. E., Chon, K. H., and Mendelson, Y. (2014). Photoplethysmograph Signal Reconstruction Based on a Novel Hybrid Motion Artifact Detection Reduction Approach. Part I: Motion and Noise Artifact Detection. *Ann. Biomed. Eng.*, 42(11):2238–2250.

Dao, D., Salehizadeh, S. M. A., Noj, Y., Chong, J. W., Cho, C., Mcmanus, D., Darling, C. E., Mendelson, Y., and Chon, K. H. (2016). A Robust Motion Artifact Detection Algorithm for Accurate Detection of Heart Rates from Photoplethysmographic Signals using Time-Frequency Spectral Features. *IEEE J. Biomed. Heal. informatics*, 21(5):1242–1253.

De Brabanter, K., Karsmakers, P., Ojeda, F., Alzate, C., De Brabanter, J., Pelckmans, K., De Moor, B., Vandewalle, J., and Suykens, J. a. K. (2003). LS-SVMlab Toolbox User's Guide. *Pattern Recognit. Lett.*, 3(February):179–202.

Empatica Inc (2017). Empatica E4 wristband. https://www.empatica.com/e4-wristband. [Online; accessed 22-August-2017].

Fischer, C., Domer, B., Wibmer, T., and Penzel, T. (2017). An algorithm for real-time pulse waveform segmentation and artifact detection in photoplethysmograms. *IEEE J. Biomed. Heal. Informatics*, 21(2):372–381.

Fukushima, H., Kawanaka, H., Bhuiyan, M. S., and Oguri, K. (2012). Estimating heart rate using wrist-type photoplethysmography and acceleration sensor while running. In *Engineering in Medicine and Biology Society (EMBC), 2012 Annual International Conference of the IEEE*, pages 2901–2904. IEEE.

Gil, E., María Vergara, J., and Laguna, P. (2008). Detection of decreases in the amplitude fluctuation of pulse photoplethysmography signal as indication of obstructive sleep apnea syndrome in children. *Biomed. Signal Process. Control*, 3(3):267–277.

Karlen, W., Kobayashi, K., Ansermino, J. M., and Dumont, G. A. (2012). Photoplethysmogram signal quality estimation using repeated Gaussian filters and cross-correlation. *Physiol. Meas.*, 33(10):1617–1629.

Kim, B. S. and Yoo, S. K. (2006). Motion artifact reduction in photoplethysmography using independent component analysis. *IEEE Trans. Biomed. Eng.*, 53(3):566–568.

Krishnan, R., Natarajan, B., and Warren, S. (2008). Analysis and detection of motion artifact in photoplethysmographic data using higher order statistics. In *Acoustics, Speech and Signal Processing, 2008. ICASSP 2008. IEEE International Conference on*, pages 613–616. IEEE.

Lai, P. and Kim, I. (2015). Lightweight wrist photoplethysmography for heavy exercise: motion robust heart rate monitoring algorithm. *Healthcare Technology Letters*, 2(1):6–11.

Lázaro, J., Gil, E., Vergara, J. M., and Laguna, P. (2014). Pulse rate variability analysis for discrimination of sleep-apnea-related decreases in the amplitude fluctuations of pulse photoplethysmographic signal in children. *IEEE J. Biomed. Heal. Informatics*, 18(1):240–246.

Lee, B., Han, J., Baek, H. J., Shin, J. H., Park, K. S., and Yi, W. J. (2010). Improved elimination of motion artifacts from a photoplethysmographic signal using a kalman smoother with simultaneous accelerometry. *Physiol Meas*, 31(12):1585–603.

Li, K. and Warren, S. (2012). A wireless reflectance pulse oximeter with digital baseline control for unfiltered photoplethysmograms. *IEEE Trans. Biomed. Circuits Syst.*, 6(3):269–278.

Li, K., Warren, S., and Natarajan, B. (2012). Onboard tagging for real-time quality assessment of photoplethysmograms acquired by a wireless reflectance pulse oximeter. *IEEE Trans. Biomed. Circuits Syst.*, 6(1):54–63.

Li, Q., Mark, R. G., and Clifford, G. D. (2008). Robust heart rate estimation from multiple asynchronous noisy sources. *Physiol. Meas.*, 29(1):15–32.

Nakajima, K., Tamura, T., and Miike, H. (1996). Monitoring of heart and respiratory rates by photoplethysmography using a digital filtering technique. *Med. Eng. Phys.*, 18(5):365–372.

Pan, H., Temel, D., and AlRegib, G. (2016). Heartbeat: Heart beat estimation through adaptive tracking. In *Biomedical and Health Informatics (BHI), 2016 IEEE-EMBS International Conference on*, pages 587–590. IEEE.

Petterson, M. T., Begnoche, V. L., and Graybeal, J. M. (2007). The effect of motion on pulse oximetry and its clinical significance. *Anesth. Analg.*, 105(6 suppl.):S78–84.

Ram, M., Madhav, K. V., Krishna, E. H., Komalla, N. R., and Reddy, K. A. (2012). A novel approach for motion artifact reduction in ppg signals based on as-lms adaptive filter. *IEEE Trans Intrum Meas*, 16:1445–1457.

Selvaraj, N., Mendelson, Y., Shelley, K. H., Silverman, D. G., and Chon, K. H. (2011). Statistical Approach for the Detection of Motion / Noise Artifacts in Photoplethysmogram. *Conf Proc IEEE Eng Med Biol Soc.*, pages 4972–4975.

Sukor, J. A., Redmond, S. J., and Lovell, N. H. (2011). Signal quality measures for pulse oximetry through waveform morphology analysis. *Physiol. Meas.*, 32(3):369–384.

Temko, A. (2017). Accurate heart rate monitoring during physical exercises using ppg. *IEEE Trans Biomed Eng.*, 64(9):2016–2024.

Tobin, R. M., Pologe, J. A., and Batchelder, P. B. (2002). A

characterization of motion affecting pulse oximetry in 350 patients. *Anesth. Analg.*, 94(1 suppl):S54–S61.

Torres, J. M. M., Ghosh, A., Stepanov, E. A., and Riccardi, G. (2016). Heal-t: An efficient ppg-based heart-rate and ibi estimation method during physical exercise. *24th European Signal Processing Conference (EUSIPCO)*.

Varon, C., Caicedo, A., Testelmans, D., Buyse, B., and Huffel, S. V. (2015). A Novel Algorithm for the Automatic Detection of Sleep Apnea From Single-Lead ECG. 62(9):2269–2278.

Yousefi, R., Nourani, M., Ostadobbas, S., and Panahi, I. (2012). A motion-tolerant adaptive algorithm for wearable photoplethysmographic biosensors. *IEEE J Biomed Health*, 18(2):670–681.